Structure−Activity Relationship for the Addition of OH to (Poly)alkenes: Site-Specific and Total Rate Constants

J. Peeters, W. Boullart, V. Pultau, S. Vandenberk, and L. Vereecken*

Department of Chemistry, University of Leuven, Celestijnenlaan 200F, B-3001 Leuven, Belgium

Received: October 24, 2006; In Final Form: January 5, 2007

A novel site-specific structure−activity relationship was developed for the site-specific addition of OH radicals to (poly)alkenes at 298 K. From a detailed structure−activity analysis of some 65 known OH + alkene and diene reactions, it appears that the total rate constant for this reaction class can be closely approximated by a sum of independent partial rate constants, k_i, for addition to the specific (double-bonded) C atoms that depend only on the stability type of the ensuing radical (primary, secondary, etc.), that is, on the number of substituents on the neighboring C atom in the double bond. The (nine) independent partial rate constants, k_i, were derived, and the predicted rate constants ($k_{OH,pred} = \Sigma k_i$) were compared with experimental $k_{OH,exp}$ values. For noncyclic (poly)alkenes, including conjugated structures, the agreement is excellent ($\Delta < 10\%$). The SAR-predicted rate constants for cyclic (poly)alkenes are in general also within <15% of the experimental value. On the basis of this SAR, it is possible to predict the site-specific rate constants for (poly)alkene + OH reactions accurately, including larger biogenic compounds such as isoprene and terpenes. An important section is devoted to the rigorous experimental validation of the SAR predictions against direct measurements of the site-specific addition contributions within the alkene, for monoalkenes as well as conjugated alkenes. The measured site specificities are within 10−15% of the SAR predictions.

Introduction

Large amounts of volatile organic compounds (VOCs) are continuously being emitted into the Earth's atmosphere, originating from both biogenic and anthropogenic sources.[1] Unsaturated hydrocarbons, including ubiquitous biogenic hydrocarbons (BVOCs) such as isoprene, the terpenes, and the sesquiterpenes, constitute a major part of the emitted organic mass. The degradation of these unsaturated VOCs in the troposphere is initiated by reactions with highly reactive species, mainly OH radicals but also O_3 and NO_3 radicals.[2−5] Reaction of OH with unsaturated VOCs is known to proceed mainly by addition to a >C═C< bond;[2] the subsequent reaction of the resulting adduct radicals with O_2 leads to organic peroxy radicals that act as intermediates in the photochemical hydrocarbon/NO-oxidation cycle, the most important source of tropospheric ozone. The lifetimes of VOCs in the atmosphere and the precise nature of the oxidation products is one of the prime research topics in atmospheric chemistry, with implications on many aspects of atmospheric chemistry. Policy makers increasingly need such information and impact studies on the chemical weather to address environmental issues. Atmospheric models describing the formation of photo-oxidants require the knowledge of all relevant processes, that is, rate constants and product distributions of the various important reaction paths. Because of the large variety of VOCs emitted in the atmosphere, it is impossible to unravel the oxidation scheme for each compound separately in laboratory experiments or by theoretical work. A solution to this is to develop structure−activity relationships (SAR) for the various reaction paths, which allows for the prediction of total rate constants and detailed primary product distributions. Given the importance of OH-addition reactions on unsaturated hydrocarbons as the initial step in VOC oxidation, a SAR for this class of reactions is an essential tool in the development of accurate chemical atmospheric models. In the reactions of OH radicals with unsaturated hydrocarbons, addition is always the dominant reaction channel. Still, there are some contributions from hydrogen abstraction reactions, which, depending on the exact structure of the hydrocarbon considered, can contribute up to 30% of the total rate coefficient.[6] In this paper, we will first derive a SAR for the addition reaction in the good first-order approximation that the total rate coefficient, k_{OH}, equals the addition rate coefficient: $k_{OH} = k_{add} + k_{abstr} \approx k_{add}$. The impact of the abstraction rate coefficient k_{abstr} on the SAR is discussed and illustrated in later sections of the paper.

Alternative existing structure−activity relationships for the addition of OH to (poly)alkenes always accord a specific reactivity to a complete C═C alkene structure or even to a complete conjugated diene structure C═C−C═C.[7−20] The total rate constant for OH + polyalkene reactions is equal to the sum of the rate constants for the reactions of OH with the various monoalkene substructures that make up the polyalkene. The impact of different substituents, conjugation effects for alkadienes, and ring strain effects for cyclic compounds are taken into account in some SARs by corrective factors for specific deviations from a given basic set of molecular templates. The underlying philosophy for considering an entire C═C moiety is the concept that an OH + alkene reaction proceeds via a π complex, as postulated by Cvetanovic more than 20 years ago;[21,22] according to this idea, the initial step amounts to a loose association of OH to the double bond, that is, to the π-electron cloud spanning the double bond:

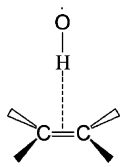

* Corresponding author. E-mail: Luc.Vereecken@chem.kuleuven.be.

10.1021/jp066973o CCC: $37.00
Published on Web 02/14/2007

TABLE 1: Reference Compounds Used to Derive the SAR Parameters; with Experimental Rate Coefficients as Listed in Reference 12

compound	$k_{OH,exp}$ (298 K)/ 10^{-11} cm^3 s^{-1}	SAR expression
ethene	0.90	$k_{OH} = 2 \times k_{prim}$
2-butene (average cis/trans)	6.02	$k_{OH} = 2 \times k_{sec}$
2,3-di-Me−2-butene	11.00	$k_{OH} = 2 \times k_{tert}$
1,3-butadiene	6.66	$k_{OH} = 2 \times k_{prim} + 2 \times k_{sec/prim}$
2,4-hexadiene (average cis/trans)	13.4	$k_{OH} = 2 \times k_{sec} + 2 \times k_{sec/sec}$
2,5-dimethyl-2,4-hexadiene	21.0	$k_{OH} = 2 \times k_{tert} + 2 \times k_{sec/tert}$
2,3-dimethyl-1,3-butadiene	12.2	$k_{OH} = 2 \times k_{prim} + 2 \times k_{tert/prim}$

The T-shaped reactant complex between OH and acetylene has been observed by infrared spectroscopy recently,[23] and recent quantum chemical and theoretical kinetic calculations on alkene + OH reactions incorporate this pre-reactive complex.[24−35] Excellent reproduction[35] of the temperature- and pressure-dependent rate coefficients is obtained by advanced theoretical kinetic methodologies using a two-transition-state model: an outer TS for reactant complex formation and an inner TS for the addition. The impact of these two TS on the addition rate coefficients depends on temperature; at room temperature both appear to be important but with a dominant effect from the inner transition state.

The development of a SAR for the addition processes of OH radicals on alkenes as a function of the entire π-bonded system (singular or conjugated) has some drawbacks. The first is that such an approach generates by default a large number of substitution patterns for which a rate coefficient must be derived. The combinatorial number of patterns increases strongly for conjugated systems; in practice, many substitution patterns are therefore grouped and a single rate coefficient is assigned to each group. The second and most important shortcoming, however, is that considering the π system as a single entity does not yield information on the relative importance of the different addition sites within the system, that is, the probability of adding on a specific carbon within a double bond. In many cases, the subsequent degradation mechanism for asymmetric alkenes depends on the specific site of OH addition, especially if (chemically activated) unimolecular isomerization reactions occur.[36−42] The relative contribution for each site is therefore often important in unraveling the oxidation mechanism and consequently assessing the impact on various issues in the chemical atmosphere.

In this work, we propose a novel structure−activity relationship for the rate coefficients at 298 K for the site-specific addition of OH radicals on double bonds, derived from the available experimental data for alkenes, polyalkenes, and conjugated alkadienes. First, we develop the SAR from its fundamental hypotheses and verify the resulting predictions on the total rate coefficient for nonconjugated alkenes against the available experimental data. The SAR is then extended within the same framework to conjugated alkadienes and tested against literature data. Experimental evidence is presented to confirm the site-specific contributions of the different addition sites as predicted using the SAR. The performance of the current SAR is then compared to other SARs available in the literature, and the fundamental hypothesis of the SAR are confronted with the available theoretical information. Finally, the most important contributions in the residual errors are discussed, and an outlook for future improvements and testing is given. Parts of this work have been published earlier;[43−45] at this time, neither allenes nor alkenes with heterosubstituents such as halogens or oxygen-bearing functional groups are considered.

SAR Development. The basic hypothesis underlying the novel, site-specific SAR that we describe here is that the kinetic bottleneck(s) in the addition pathways for addition of OH on a double bond contain a separable and independent contribution of the different addition sites, that is, that each of the carbons in the double bond has an individual effect on the addition process, uncorrelated to the other addition site within that double bond, and in proportion to the probability of adding to that specific site within the double bond. As the various possible addition processes of OH to the n double-bonded C atoms of the (poly)alkene are considered with an independent contribution, the total rate constant, k_{OH}, is the sum of partial rate constants, k_i, of addition on the specific sites i:

$$k_{OH} = \sum_{i}^{n} k_i$$

Each of the specific sites, i, corresponds to an individual double-bonded C atom (C_a) on which OH adds; its partner carbon in the double bond, C_b, is to be considered a separate, independent addition site. This is different from other SARs that consider the set of two carbons in the double bond as the smallest entity. When hypothesizing that the site-specific addition contributions are separable, we do not propose a specific mechanism for addition. Indeed, for the purpose of this paper it is not relevant whether the addition occurs through one of several independent transition states or through one of several rate-determining channels involving a collective pre-reactive π complex. Nonetheless, we will confront this hypothesis with the available mechanistic data in a later section.

A second hypothesis is that the magnitude of a site-specific rate constant, k_i, for addition is determined solely by the stability type of the product radical being formed. For addition on a carbon C_a, the nature of the adduct radical formed is determined by the environment of the partner carbon C_b, that is, the substitutions X_3 and X_4 on that carbon: the radical site is either primary (both X_3 and X_4 are hydrogen), secondary (one of X_3 and X_4 are H), or tertiary (neither X_3 nor X_4 are H):

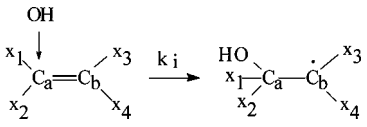

A direct implication of the hypothesis above is, because there are only three types of adduct radicals for monoalkenes and nonconjugated polyalkenes, that there are only three partial site-specific rate constants, k_i, depending on the stabilization type of the resulting hydroxy-adduct radical: k_{prim}, k_{sec}, and k_{tert} for primary, secondary, and tertiary product radicals, respectively. Provided the above working hypotheses holds, these three partial site-specific rate constants should enable one to predict the total rate coefficients and site-specific contributions for all regular alkenes:

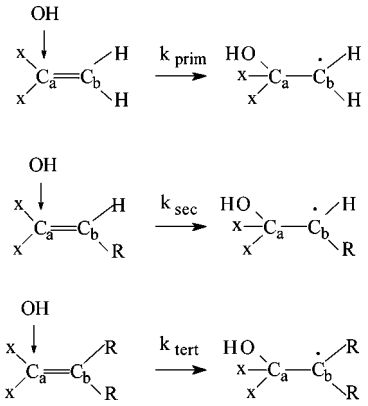

It follows directly from our hypotheses that the values of k_{prim}, k_{sec}, and k_{tert} can be derived, respectively, from the total rate constants[12,46] (high-pressure limits at 298 K) for OH addition to the symmetric alkenes ethene, 2-butene (we use an average over cis and trans forms), and 2,3-dimethyl-2-butene (see Table 1) where only a primary, secondary, or tertiary product radical can arise:

$$k_{prim} = {}^1/_2 k_{OH}^{\infty}\,(\text{ethene}) = 0.45 \times 10^{-11}\ \text{cm}^3\ \text{molecule}^{-1}\ \text{s}^{-1}$$

$$k_{sec} = {}^1/_2 k_{OH}^{\infty}\,(\text{2-butene}) = 3.0 \times 10^{-11}\ \text{cm}^3\ \text{molecule}^{-1}\ \text{s}^{-1}$$

$$k_{tert} = {}^1/_2 k_{OH}^{\infty}\,(\text{2,3-dimethyl-2-butene}) = 5.5 \times 10^{-11}\ \text{cm}^3\ \text{molecule}^{-1}\ \text{s}^{-1}$$

The complete set of site-specific k_i needed to describe OH addition to (poly)alkenes is listed in Table 2.

Validation of the Basic Hypotheses. To validate the above-stated site-specific SAR hypothesis, the predicted total rate coefficients, k_{OH}, calculated as the sums of the site-specific addition rate coefficients $k_{OH} = \Sigma k_i$, and using only the three k_i given above, were compared with the experimental overall k_{OH} values for 27 noncyclic alkenes and nonconjugated alkadienes, 9 monocyclic structures, and 13 bi- or tricyclic compounds (see Tables 3 and 4, and Figures 1 and 2), that is, for all relevant compounds for which data were found in the literature. Such a comparison assumes that the overall rate of reaction is determined solely by OH addition on the unsaturated double bonds. Alkenes are known to react predominantly with the OH radical by addition, but we will discuss the systematic bias induced by this assumption in the comparison section later. The relative deviations from the experimental data were calculated as abs($(k_{SAR} - k_{OH})/k_{OH}$)); note that the SAR developed in this work does not contain any adjustable parameters. For the noncyclic, nonconjugated alkenes, the SAR prediction agrees quasi-perfectly with the experimental data; the average deviation of 9% and a largest deviation of 32% is comparable to the uncertainty on the measurements. For monocyclic structures, including compounds with strained rings, the average deviation is about 13% (see Table 3 and Figure 1). The SAR predictions for the addition rate coefficient for the bicyclic compounds (see Table 4 and Figure 2) corresponds on average within 24% of the experimental total rate coefficient of these compounds; the set of bicyclic compounds includes mostly terpenenes and sesquiterpenes. Some notable large deviations exist for sabinene, α-pinene, and bicyclo[2.2.2]-2-octene (−49%, +63%, and +47%, respectively). Aside from these very few exceptions for strained bicyclic compounds, our SAR predicts the experimental rate coefficients for the diverse test set of 47 compounds surprisingly well (Figure 4), considering that it contains no adjustable parameters and is derived solely from the experimental rate data for only three symmetric reference compounds. This strongly supports a number of conclusions concerning the basic tenets of our SAR as outlined above: (*i*) the rate of reaction can be described as a sum of independent site-specific rate coefficients, (*ii*) the rate of addition can be described by only three parameters determined solely by the substitution on the product radical carbon, and of course (*iii*) the rate of reaction is determined mostly by OH addition. A later section in this paper will discuss some systematic and some specific deviations between experiment and SAR in more detail.

TABLE 2: SAR Parameters (10^{-11} cm^3 s^{-1}) for Addition of OH on a (Poly)alkene

$k_{prim} = 0.45$	$k_{sec} = 3.0$	$k_{tert} = 5.5$
	$k_{sec/prim} = 3.0$	$k_{tert/prim} = 5.7$
	$k_{sec/sec} = 3.7$	$k_{tert/sec} = 8.3$[a]
	$k_{sec/tert} = 5.0$	$k_{tert/tert} = 9.9$[a]

[a] Not derived directly from experimental data (see the text).

TABLE 3: SAR Predictions for Linear, Branched, or Monocyclic Nonconjugated (Poly)alkenes

compound	SAR expression $k_{OH,pred} =$	$k_{OH,exp}$[a] 10^{-11}	$k_{OH,pred}$[c] 10^{-11}
ethene	$k_{prim} + k_{prim}$	0.90	(0.90)
propene	$k_{prim} + k_{sec}$	2.63	3.46
1-butene	$k_{prim} + k_{sec}$	3.14	3.46
1-pentene	$k_{prim} + k_{sec}$	3.5	3.46
1-hexene	$k_{prim} + k_{sec}$	3.7	3.46
1-heptene	$k_{prim} + k_{sec}$	4.0	3.46
2-butene	$k_{sec} + k_{sec}$	6.02[b]	(6.02)
2-pentene	$k_{sec} + k_{sec}$	6.6[b]	6.02
trans-2-heptene	$k_{sec} + k_{sec}$	6.8	6.02
2-methyl-propene	$k_{prim} + k_{tert}$	5.14	5.95
3-methyl-1-butene	$k_{prim} + k_{sec}$	3.18 (2.95)[d]	3.46
2-methyl-1-butene	$k_{prim} + k_{tert}$	6.1	5.95
2-methyl-2-butene	$k_{sec} + k_{tert}$	8.69	8.51
2-methyl-1-pentene	$k_{prim} + k_{tert}$	6.3	5.95
2-methyl-2-pentene	$k_{sec} + k_{tert}$	8.9	8.51
trans-4-methyl-2-pentene	$k_{sec} + k_{sec}$	6.1	6.02
2,3-dimethyl-2-butene	$k_{tert} + k_{tert}$	11.0	(11.00)
3,3-dimethyl-1-butene	$k_{prim} + k_{sec}$	2.8	3.46
2,3-dimethyl-2-pentene	$k_{tert} + k_{tert}$	10.3	11.00
trans-4,4-dimethyl-2-pentene	$k_{sec} + k_{sec}$	5.5	6.02
trans-4-octene	$k_{sec} + k_{sec}$	6.9	6.02
1,5-hexadiene	$k_{prim} + k_{sec} + k_{sec} + k_{prim}$	6.2	6.91
2-methyl-1,5-hexadiene	$k_{prim} + k_{tert} + k_{sec} + k_{prim}$	9.6	9.40
2,5-dimethyl-1,5-hexadiene	$k_{prim} + k_{tert} + k_{tert} + k_{prim}$	12.0	11.89
1,4-pentadiene	$k_{prim} + k_{sec} + k_{sec} + k_{prim}$	5.3	6.91
trans-1,4-hexadiene	$k_{prim} + k_{sec} + k_{sec} + k_{sec}$	9.1	9.46
2-methyl-1,4-pentadiene	$k_{prim} + k_{prim} + k_{tert} + k_{sec}$	7.9	9.40
cyclopentene	$k_{sec} + k_{sec}$	6.7	6.02
cyclohexene	$k_{sec} + k_{sec}$	6.77	6.02
cycloheptene	$k_{sec} + k_{sec}$	7.4	6.02
1-methylcyclohexene	$k_{sec} + k_{tert}$	9.4	8.51
d-limonene	$k_{prim} + k_{sec} + k_{tert} + k_{tert}$	16.4	14.44
1,4-cyclohexadiene	$k_{sec} + k_{sec} + k_{sec} + k_{sec}$	9.95 (9.3)[d]	12.04
γ-terpinene	$k_{sec} + k_{sec} + k_{tert} + k_{tert}$	17.7	17.02
terpinolene	$k_{sec} + k_{tert} + k_{tert} + k_{tert}$	22.5	19.51
α-humulene	$4 \times k_{sec} + 2 \times k_{tert}$	29.3	23.04

[a] Listed in ref 12. [b] Average of cis and trans conformers. [c] Values in parentheses are used to derive the SAR (see the text). [d] Value in parentheses is the addition rate coefficient, $k_{add,exp}$, determined from the experimental total rate coefficient, $k_{OH,exp}$, and the fraction of H abstraction (see the text).

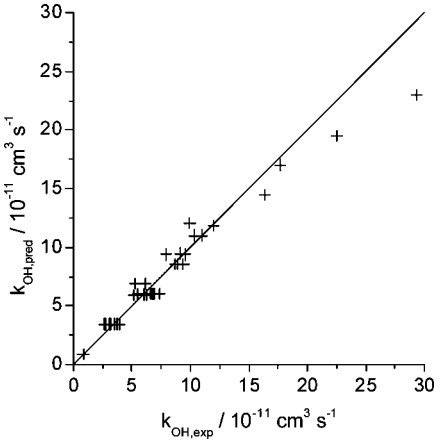

Figure 1. Linear, branched, and monocyclic nonconjugated (poly)-alkenes: comparison between the experimental total rate coefficient for reaction with OH, $k_{OH,exp}$, against the SAR predictions, $k_{OH,pred}$. The solid line represents the ideal 1:1 comparison.

TABLE 4: SAR Predictions for Bicyclic Nonconjugated (Poly)alkenes

compound	SAR expression $k_{OH,pred}$ =	$k_{OH,exp}$ [a] 10^{-11}	$k_{OH,pred}$ 10^{-11}
β-pinene	$k_{prim} + k_{tert}$	7.43	5.95
Δ^3-carene	$k_{sec} + k_{tert}$	8.8	8.51
Δ^2-carene	$k_{sec} + k_{tert}$	8.0	8.51
α-pinene	$k_{sec} + k_{tert}$	5.23	8.51
α-cedrene	$k_{sec} + k_{tert}$	6.7	8.51
longifolene	$k_{prim} + k_{tert}$	4.7	5.95
α-copaene	$k_{sec} + k_{tert}$	9.0	8.51
bicyclo[2.2.1]-2-heptene	$k_{sec} + k_{sec}$	4.9	6.02
bicyclo[2.2.1]-2,5-heptadiene	$k_{sec} + k_{sec} + k_{sec} + k_{sec}$	12.0	12.04
bicyclo[2.2.2]-2-octene	$k_{sec} + k_{sec}$	4.1	6.02
camphene	$k_{prim} + k_{tert}$	5.3	5.95
sabinene	$k_{prim} + k_{tert}$	11.7	5.95
β-carryophyllene	$k_{prim} + k_{sec} + k_{tert} + k_{tert}$	19.7	14.46

[a] Listed in ref 12.

Extension to Conjugated Dienes. A similar reasoning as described above applies for OH addition to conjugated dienes $C_a{=}C_b{-}C_c{=}C_d$, but here one must account for possible resonance stabilization of the radical formed after addition of OH. This resonance stabilization only occurs when the OH radical adds to one of the outer C atoms of the conjugated diene. An example is

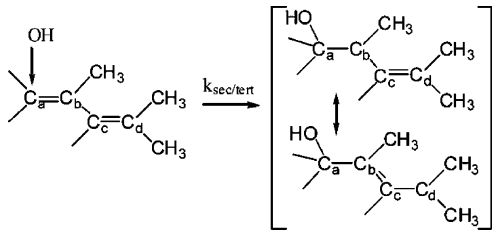

where $k_{sec/tert}$ denotes the partial rate constant for addition to the specific site above resulting in a resonance stabilized secondary ↔ tertiary radical. As before, we hypothesize that the site-specific rate of reaction depends on the stability of the product radical; for resonance-stabilized radicals, this therefore depends on the substitution of the two radical sites, C_b and C_d, in the resonance structures. In general, there are six resonance cases and hence six partial rate constants for conjugated dienes: for addition on C_a, the first radical site, C_b (the second carbon of the double bond whereon the reaction occurs) is either a secondary (R_1 = H) or tertiary radical site (R_1 = alkyl). The second radical site, C_d, is reached by shifting the conjugated double bond and is a primary (R_2/R_3 = H), secondary (R_2 = H, R_3 = alkyl), or tertiary site (R_2/R_3 = alkyl):

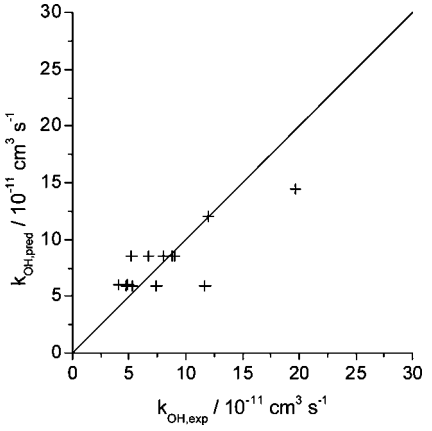

Figure 2. Bicyclic nonconjugated (poly)alkenes: comparison between the experimental total rate coefficient for reaction with OH, $k_{OH,exp}$, against the SAR predictions, $k_{OH,pred}$. The solid line represents the ideal 1:1 comparison.

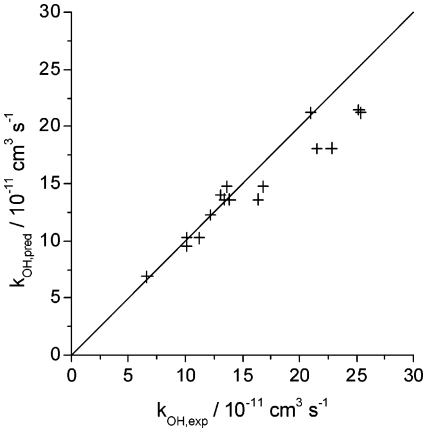

Figure 3. Conjugated alkadienes: comparison between the experimental total rate coefficient for reaction with OH, $k_{OH,exp}$, against the SAR predictions, $k_{OH,pred}$. The solid line represents the ideal 1:1 comparison. For α-phellandrene and α-terpinene, the experimental addition rate coefficients, $k_{add,exp}$, corrected for H abstraction were used (see discussion).

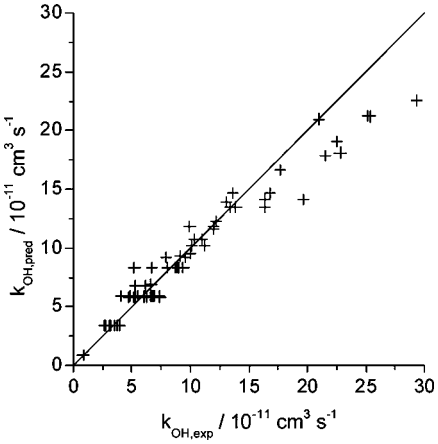

Figure 4. Comparison between the experimental total rate coefficient for reaction with OH, $k_{OH,exp}$, against the SAR predictions, $k_{OH,pred}$. The solid line represents the ideal 1:1 comparison. The experimental addition rate coefficients $k_{add,exp}$ corrected for H abstraction were used for α-phellandrene and α-terpinene; sabinene was omitted (see discussion).

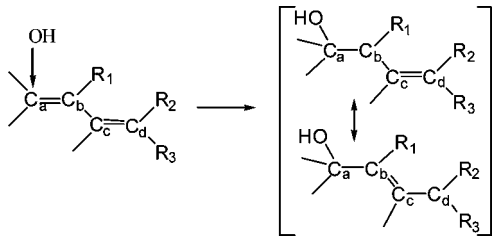

The six additional k_i were evaluated from experimental data on the overall k_{OH} of some conjugated alkadienes and are denoted as $k_{first/second}$ to indicate the stability types of the first and second radical sites C_b and C_d, respectively. The values for $k_{sec/prim}$, $k_{sec/sec}$, $k_{sec/tert}$, and $k_{tert/prim}$ were obtained (see Table 1) from the experimental values of 1,3-butadiene, *cis*- and *trans*-2,4-hexadiene (averaged), 2,5-dimethyl-2,4-hexadiene, and 2,3-dimethyl-1,3-butadiene. For the determination of $k_{tert/sec}$ and $k_{tert/tert}$, the recommended values of Atkinson were used.[2] These six site-specific rate coefficients for conjugated alkenes supplement k_{prim}, k_{sec}, and k_{tert} for nonconjugated alkenes; the complete set of nine k_i needed to describe OH addition to (poly)alkenes is listed in Table 2. The rate constants for conjugated structures become larger with increasing substitution both on the first and second product radical site. It is interesting that increased substitution of the product radical in conjugated alkenes does not effect the rate of addition as much as would be expected from the energy difference imparted by the radical delocalisation stabilization. In fact, the site-specific rates of reaction k_{sec} and $k_{sec/prim}$ are nearly identical, as are k_{tert} and $k_{tert/prim}$. The transition state for conjugated alkenes is not affected as much as by electron delocalization as the product radical is because in the early TS the pertaining electrons are still involved in the carbon−oxygen bond being formed and the C=C bond being broken and are not free yet for delocalization. Delocalization of the product radical electron is a rather late effect occurring mostly after the TS and does not change the characteristics of the transition state extensively. Hyperconjugation and induction stabilization act on the first radical site at all times, regardless of the freedom of movement of the radical electron, and are therefore much more effective in altering the transition-state characteristics. This is also the reason why we cannot consider, for example, secondary ↔ tertiary and tertiary ↔ secondary resonance structures as identical: the first radical site, in the β position to the addition site, has a more dominant impact, whereas the substitution around the second radical site in the δ position has a minor impact. Analogous effects by late delocalization stabilization were discussed earlier for H abstraction by OH radicals in strained cyclic compounds.[47]

To test the SAR hypotheses and the site-specific rate coefficients for conjugated alkenes, we again compare experimental total rate coefficients for addition with the sum of the rates coefficients over all of the different sites, $k_{OH} = \Sigma k_i$ (see Table 5 and Figure 3). The set consists of 16 conjugated dienes, and the experimental total rate coefficients are reproduced on average within 11%. Most of the deviation is caused by the compounds α-phellandrene and α-terpinene (>40% underprediction of k_{OH}); excluding these compounds improves the average deviation to about 7%, directly comparable to the experimental errors. This indicates clearly that the total rate coefficient for the reaction of OH radicals with alkenes is well predicted by the site-specific addition rate coefficients listed in Table 2. Earlier experimental work by our group[6] examined the reasons for the severe underestimation for α-phellandrene and α-terpinene. It was found that significant H abstraction occurred in the reaction of these compounds with OH, with contributions of 27 ± 10% and 30 ± 7%, respectively. Hence, simply equating the total rate coefficient k_{OH} to the addition rate coefficient k_{add} as predicted by our SAR is not valid for these compounds. The experimental rate coefficient for addition can be obtained by subtracting the fraction of H abstraction from the total experimental rate coefficient for the reaction with OH. For α-phellandrene, with $k_{OH} = (3.1 \pm 0.4) \times 10^{-10}$ cm^3 s^{-1} and 27% H abstraction, this leads to a total addition rate coefficient of $k_{add} = 2.3 \times 10^{-10}$ cm^3 s^{-1}. For α-terpinene, with $k_{OH} = (3.6 \pm 0.4) \times 10^{-10}$ cm^3 s^{-1} and 30% H abstraction, this results in $k_{add} = 2.5 \times 10^{-10}$ cm^3 s^{-1}.[6] These corrections for H abstraction account for the bulk of the earlier difference with the SAR predictions of 1.8×10^{-10} and 2.1×10^{-10} cm^3 s^{-1} for α-phellandrene and α-terpinene, respectively. These latter predictions are within ~25% of the corrected experimental values and within the experimental uncertainty even if they still seem to underestimate the addition rate coefficient somewhat. The effects of H abstraction on the general quality of our SAR predictions (Figure 4) is discussed in more detail below.

Experimental Validation. The most important improvement of the SAR described in this work compared to earlier work is the prediction of site-specific rate coefficients as opposed to total rate coefficients per double bond. Comparing the sum of the SAR-predicted site-specific k_i against the experimental total rate coefficients for addition is a good test for the overall validity of the SAR but does not guarantee a priori that the individual site-specific addition rate coefficients are predicted correctly: the relative importance of the different addition carbons might change after the rate-determining TS is passed, or the agreement might be fortuitous. To fully validate the site specificity of the SAR, we therefore need additional, more stringent tests comparing the contributions of the individual site-specific rate coefficients, $k_i/\Sigma k_i$, in the total rate coefficient for addition against experimental data.

To this end, the primary hydroxy adduct distributions of the reaction of OH radicals with a number of asymmetric (poly)-alkenes were measured directly using a multistage flow reactor technique in combination with molecular beam sampling mass spectrometry (MBMS). The apparatus used has been described elsewhere[6] and is described only briefly here. The setup consists of a conventional fast-flow reactor consisting of a cylindrical quartz tube (internal diameter 2.7 cm) equipped with a microwave-discharge side arm and a set of three axially movable central injector tubes. The positioning of the central injector tube's outlets creates different reaction zones, the length of which can be modified independently; this allows for the variation of the reaction times in each of the reaction zones. The gas at the reactor exit was sampled through a 0.3 mm pinhole in the tip of a thin-walled quartz cone, giving access to the first of three differentially pumped vacuum chambers. The resulting molecular beam is mechanically modulated to allow phase-sensitive detection, and, after passing an axial, high-yield electron-impact ionizer, is analyzed by a high-transmittance Extranuclear Laboratories quadrupole mass spectrometer, equipped with an off-axis ion multiplier. Phase-sensitive detection rejects any contribution of ions from the background gas. Helium was used as reactor carrier gas throughout, with a total pressure of 2−5 Torr; flow speeds were in the 1100−1700 cm s^{-1} range.

Hydroxyl radicals were generated in the reaction of H atoms with NO_2; the H atoms ([H] ≈ 2×10^{13} molecules cm^{-3}) were created in an upstream microwave discharge through a flow of 5% H_2 in He, at a total pressure of 2−5 Torr, and then mixed with an excess of NO_2 ([NO_2] ≈ 6×10^{13} molecules cm^{-3}) in the first reactor stage. The concentration of added NO_2 required

TABLE 5: SAR Predictions for Conjugated Polyalkenes

compound	SAR expression $k_{OH,pred}$ =	$k_{OH,exp}$ [a] 10^{-11}	$k_{OH,pred}$ [d] 10^{-11}
cis-1,3-pentadiene	$k_{prim} + k_{sec} + k_{sec/sec} + k_{sec/prim}$	10.1	10.15
2-methyl-1,3-butadiene	$k_{prim} + k_{prim} + k_{sec/prim} + k_{tert/prim}$	10.1	9.55
trans-1,3-hexadiene	$k_{prim} + k_{sec} + k_{sec/sec} + k_{sec/prim}$	11.2	10.15
2-methyl-1,3-pentadiene	$k_{prim} + k_{sec} + k_{sec/prim} + k_{tert/sec}$	13.6	14.76
4-methyl-1,3-pentadiene	$k_{prim} + k_{tert} + k_{sec/tert} + k_{sec/prim}$	13.1	13.95
1,3-cyclohexadiene	$k_{sec} + k_{sec} + k_{sec/sec} + k_{sec/sec}$	16.4 (14.2)[b]	13.40
1,3-cycloheptadiene	$k_{sec} + k_{sec} + k_{sec/sec} + k_{sec/sec}$	13.9	13.40
β-phellandrene	$k_{prim} + k_{sec} + k_{tert/sec} + k_{sec/prim}$	16.8	14.76
myrcene	$2 \times k_{prim} + k_{sec} + k_{tert} + k_{sec/prim} + k_{tert/prim}$	21.5	18.06
ocimene	$k_{prim} + 2 \times k_{sec} + k_{tert} + k_{sec/sec} + k_{tert/prim}$	25.2	21.31
α-phellandrene	$k_{sec} + k_{sec} + k_{tert/sec} + k_{sec/sec}$	31.3 (22.8)[b]	18.01
α-terpinene	$k_{tert} + k_{tert} + k_{sec/tert} + k_{sec/tert}$	36.3 (25.4)[b]	21.00
1,3-butadiene	$k_{prim} + k_{prim} + k_{sec/prim} + k_{sec/prim}$	6.7	(6.9)
2,4-hexadiene	$k_{sec} + k_{sec} + k_{sec/sec} + k_{sec/sec}$	13.4[c]	(13.4)
2,3-dimethyl-1,3-butadiene	$k_{prim} + k_{prim} + k_{tert/prim} + k_{tert/prim}$	12.2	(12.2)
2,5-dimethyl-2,4-hexadiene	$k_{tert} + k_{tert} + k_{sec/tert} + k_{sec/tert}$	21.0	(21.0)

[a] Listed in ref 12. [b] Value in parentheses is the addition rate coefficient, $k_{add,exp}$, determined from the experimental total rate coefficient, $k_{OH,exp}$, and the fraction of H abstraction (see the text). [c] Average of cis and trans conformers. [d] Values in parentheses are used to derive the SAR (see the text).

to ensure quantitative conversion of the H atoms to OH radicals was determined by titration experiments monitoring the NO coproduct concentration. Vibrationally excited OH radicals ($v = 1$, $v = 2$) are rapidly quenched in collisions by H and NO_2.[48] Some experiments were conducted with added CF_4 acting as an efficient collider to further enhance the quenching rates. In these experiments, no differences were found in the relative height of the measured mass spectrometric peaks compared to the CF_4-free experiments, indicating complete quenching even without CF_4; the results described below are without the CF_4 additive to avoid interference of the CF^+ fragmentation peak at $m/e = 31$.

The thermalized OH radicals were mixed in the second reactor stage with a large excess of alkene ([OH] $\approx 10^{13}$ molecules cm^{-3}, [alkene] $> 10^{14}$ molecules cm^{-3}) in a He flow, ensuring quantitative reaction of the OH radicals with the alkene to form the (various) primary hydroxy adducts, within a few milliseconds. Wall losses of OH radicals were minimized by passivating the quartz reactor walls and inner tubes with HF. The resulting hydroxy adducts were sampled a few milliseconds after their formation and analyzed by measuring their mass spectra as generated at a moderate ionizing electron energy of 30 eV. For all alkenes investigated here, the OH additions are known to already be in their high-pressure limit at the experimental pressures of 2−5 Torr,[49] such that redissociation of the (initially hot) hydroxy adducts can be considered negligible. Likewise, the hydroxy adducts are not expected to undergo significant secondary reactions prior to sampling: oxygen is entirely absent, (hydroxyl)alkyl radicals react negligibly slow with alkenes, and the concentration of the other potentially reactive species, NO_2 and NO, is sufficiently low. The results described here were found to be insensitive to the reaction time allowed: typical reaction times employed in the reaction zones are about 4−6 ms, but varying the reaction times from 2 to 10 ms did not change the results significantly. The lack of time dependence indicates that the reactions are complete for the purpose of this experiment both in the preparation and the reaction zones, that mixing between the different gas flows is complete, and that no significant secondary reaction of the hydroxy adducts occurs. At an ionizing electron energy of 30 eV, ionization occurs by ejection of the radical electron, forming β-hydroxy cations that fragment in a number of ways, thus generating a specific mass spectrum. The electron impact energy is sufficiently high to ensure near-complete fragmentation, but low enough that only the energetically most favored channels will dominate.

By performing the described experiment on the symmetric alkenes 2-butene and tetramethylethene, where only one type of primary hydroxy adduct can be formed, we found[50,51] that there are three dominant fragmentation routes for β-hydroxy cations: direct fragmentation and fragmentation after a 1,2- or 1,3-hydrogen shift; these channels lead to the most stable products characterized by the formation of at least one additional π bond:

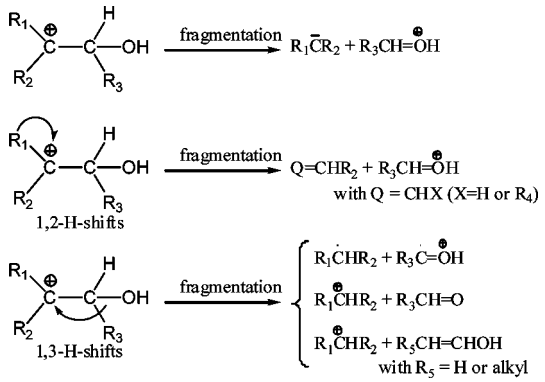

The major fragment ions of any hydroxy-alk(en)yl can be predicted from these predominant fragmentation pathways. Though the relative importance of the individual fragmentation channels for a given hydroxy radical cannot be evaluated a priori, the sum over all of the possible fragment ions is proportional to the total amount of parent radical. The contribution of fragmentation routes not included above is sufficiently small to consider them negligible with respect to the other uncertainties in the experiments.

For hydroxy adducts formed in the reaction of OH radicals with an asymmetric alkene, each site-specific adduct will have a different fragmentation spectrum with different contributions of the fragmentation routes and (usually) different fragment ions. In the ideal case, each fragment ion observed in the mass spectrum can be assigned uniquely as originating from one of the possible hydroxy adducts. Then, the sum over the site-specific fragment ions corresponds to the contribution of the site-specific adduct in the total fragment ion formation. Ion masses common to different adduct radicals cannot be assigned

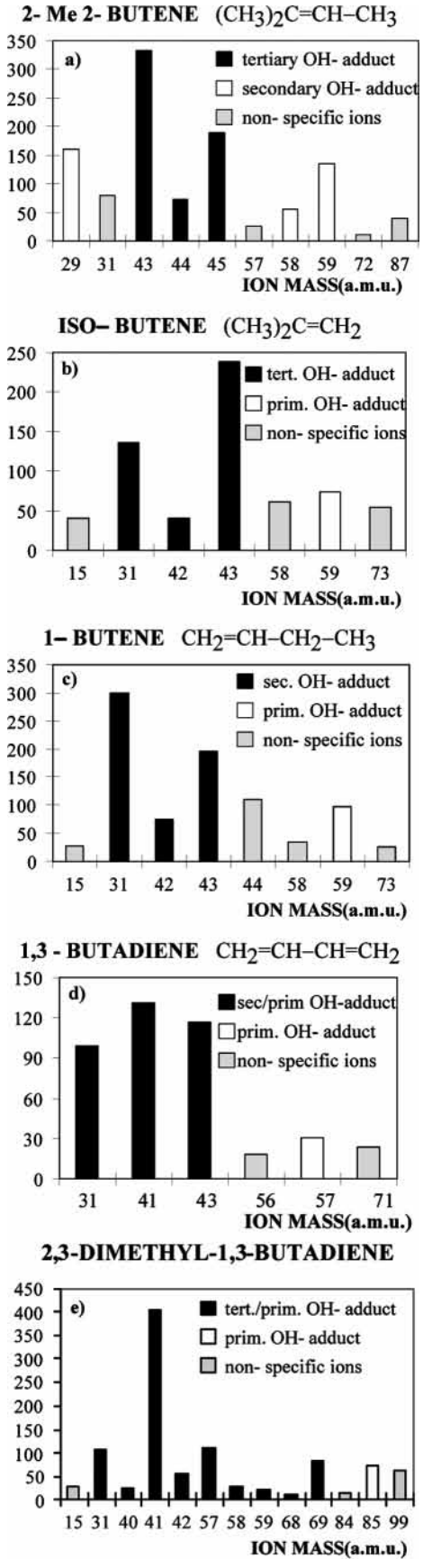

Figure 5. Fragmentation mass spectra (30 eV) of the mixture of OH-adduct radicals formed in the reaction of the alkene with OH.

uniquely and correspond to a fraction of the adduct formation for which the addition site cannot be determined; this introduces an additional uncertainty in the product analysis. Even for the selected compounds studied here, 5−10% of the fragment ions are not site-specific; this nonspecific fraction was found to be the largest contribution to the uncertainty on the product analysis and is the limiting factor in the general application of the current experimental methodology to a wider range of compounds.

Following our analysis of the two symmetric alkenes 2-butene and tetramethylethene, we applied the same methodology to three asymmetric alkenes: 2-Me-2-butene, isobutene, and 1-butene, in order to determine their primary product distributions. In addition, we applied the same methodology to two symmetric conjugated alkadienes, 1,3-butadiene and 2,3-di-Me-1,3-butadiene, so as to examine the contribution of allyl-resonance-stabilized adducts versus the regular addition sites. Figure 5 shows the mass spectra as measured after OH addition to each of these compounds. The fragmentation channels for each of the hydroxy adducts were also predicted using the aforementioned predominant fragmentation routes; comparison of the expected fragment ion masses and the measured peak heights allowed us to assign each peak to either of the addition sites, or to determine that it was nonspecific to any site. This analysis is comparatively straightforward but rather lengthy and is not given in detail here; an explicit list of predicted fragment ions and their individual formation channels can be found in refs 50 and 51. Table 6 shows the experimental product distribution, each averaged over a set of three experiments, in comparison with the SAR predictions. The predicted distributions agree with the experimental data within 5−10% (absolute) for both the monoalkenes and conjugated alkadienes, well within the experimental error. For the 2,3-di-Me-1,3-butadiene + OH reaction, the large peak on mass 41 could in principle be formed from both the primary and the tertiary/primary additions, and performing the site-specificity analysis disregarding this peak leads to an 89:11 ratio for $k_{\text{tert/prim}}/k_{\text{prim}}$, in good agreement with the SAR prediction of 93:7. However, because the largest product peak is neglected in calculating the experimental ratio the uncertainty is quite large, 89^{+7}_{-50}:11^{+50}_{-7}. However, the measurements for unsubstituted 1,3-butadiene[50] indicate that the likelihood of mass 41 to originate from the primary radical adduct is fairly small because the competing direct elimination of singlet CH_2 is significantly more favorable. Hence, the peak for mass 41 is most likely predominantly originating from the tert/prim adduct; such an assignment yields a 95:5 ratio for $k_{\text{tert/prim}}/k_{\text{prim}}$, close to our earlier experimental result and the SAR predictions but with a significantly reduced uncertainty margin: 95^{+1}_{-7}:5^{+7}_{-1}.

The results described in this section (Table 6) confirm by direct measurements that the ratios of the site-specific rate coefficients are in accord with the structure−activity relationship described in this work. In combination with the good reproduction of virtually all experimental k_{OH} as the sum of the site-specific Σk_i, the experiments qualify the basic hypotheses of the SAR and the values of its parameters, even though each site-specific rate coefficient is not examined explicitly in the experiments.

We also performed a different set of experiments to further validate the SAR by adding Br_2 ($[Br_2] \approx 2 \times 10^{15}$ molecules cm^{-3}) to the reaction mixture after the formation of the β-hydroxy-alkyl radicals using an additional, third central injection tube, yielding stable bromo-alcohols:

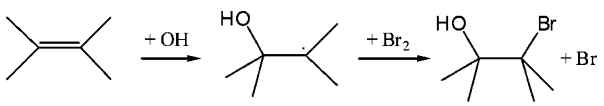

Resonance-stabilized hydroxy-alkyl radicals formed in the reaction of conjugated alkadienes with OH can yield two different bromo-alcohols:

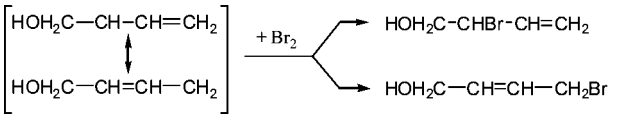

The fragmentation mass spectrum of the mixture of the bromo-alcohols was then measured after sampling and ionization; this mass spectrum is a superposition of the mass spectra of each of the different bromo-alcohols formed in the flow tube. The mass spectra for the individual bromo-alcohols are characteristic fingerprints with constant relative intensities $f_m = I_m/I_{tot}$ for each mass peak m, and the total signal strength $I_{tot} = \Sigma I_m$ is linearly dependent on the concentration $[X]$ of the compound considered: $I_m \sim f_m[X]$ and $I_{tot} \sim \Sigma f_m[X]$. Also, all of the bromo-alcohols formed are isomers, with virtually identical ionization cross sections and hence an identical total signal strength, I_{tot}, for identical concentrations. Therefore, the measured mass spectrum for the bromo-alcohol mixture is a linear combination of these fingerprint spectra with, for each mass m, contributions I_m proportional to the concentration $[X]$ or the mole fraction x_X of bromo-alcohol X :

$$I_{m,tot} \sim f_{m,A}[A] + f_{m,B}[B] + f_{m,C}[C] + ...$$

$$I_{m,tot} \sim f_{m,A}x_A + f_{m,B}x_C + f_{m,C}x_C + ...$$

The relative peak intensities, f_m, can be determined directly from fragmentation spectra of the pure bromo-alcohols, either available commercially or synthesized in our lab. Consequently, one can determine the relative concentration of each of the bromo-alcohols, and hence the relative contribution of each of the OH addition sites in the alkene, from a fitting procedure on the relative contributions, x_X, against a sufficiently large set of linear equations for mass peak intensities. We opted to include more mass peak intensities, $I_{m,tot}$, than strictly necessary because a fitting procedure on this overdetermined set of equations reduces the impact of the experimental uncertainties on individual peak intensities and gives an indication of the uncertainty on the site-specific contributions of the OH addition. Note that this method does not require that the formation channels of the individual fragment ions are known, in contrast to the earlier methodology, nor does it need the absolute concentrations of the bromo-alcohols. However, it relies on the availability of pure samples of all of the bromo-alcohols formed because one needs to determine the fingerprint relative intensities, f_m, by measuring the fragmentation spectra directly. Very few of the bromo-alcohols are available commercially and usually only in (calibrated) mixtures. Synthesis and purification of bromo-alcohols is rather troublesome, often compounded further by fast decomposition of the samples within hours or days. This lack of stability also suggests that some of the chemically activated intermediates within the experimental setup might undergo isomerization or fragmentation reactions, making comparison to the reference mass spectra inaccurate. These difficulties led to rather large uncertainties on the site specificity determined, especially for the sites with the lowest contributions.

We applied this technique to the 1,3-butadiene + OH reaction, which can yield three bromo-alcohols: CH_2═$CH-CHOH-CH_2Br$ (adduct A) from addition on the central hydrocarbons, and CH_2═$CH-CHBr-CH_2OH$ (B) or CH_2Br-CH═$CH-CH_2OH$ (C) after allyl-resonance-enhanced addition on the outer carbons. Their reference fragmentation mass spectra, yielding $f_{m,X}$, were measured at 5 Torr with an electron impact energy of 30 eV; the concentration of the bromo-alcohols was of the order of 5×10^{12} molecules cm^{-3}. Compound A was obtained from Pfaltz and Bauer; compounds B and C were synthesized and purified as described in ref 50. Fitting the mass spectrum of the bromo-alcohol mixture formed in the 1,3-butadiene + OH + Br_2 reaction against these reference spectra, using the mass peaks at m/e = 31, 41, 43, and 57, a ratio A/(B + C) of −2.5%:102.5% was found, with a fairly large statistical error of ±16% (absolute) but qualitatively supporting the 13%:87% SAR-predicted dominance of $k_{sec/prim}$ over k_{prim}. Additional experiments using propene yielded results with even larger uncertainties; the difficulties in obtaining or synthesizing the pure samples of the thermally unstable bromo-alcohols, and some evidence that chemically activated reactions are distorting the mass spectra of the bromo-alcohols in the reaction mixture relative to their reference spectra, caused us to abandon this approach.

TABLE 6: Comparison of the Experimental Branching Ratios Against the SAR Predictions

compound	branching	experimental ratio	SAR prediction
2-Me-2-butene	k_{tert}/k_{sec}	66^{+7}_{-10}:34^{+10}_{-7}	65:35
isobutene	k_{tert}/k_{prim}	85:15 (±10)[a]	92:8
1-butene	k_{sec}/k_{prim}	85:15 (±10)[a]	87:13
1,3-butadiene	$k_{sec/prim}/k_{prim}$	87.5^{+2}_{-5}:12.5^{+5}_{-2}	87:13
2,3-diMe-1,3-butadiene	$k_{tert/prim}/k_{prim}$	95^{+1}_{-7}:5^{+7}_{-1} [b]	93:7

[a] Value in parentheses: approximate error margin. [b] Ratio when assigning the peak at mass 41 to the tert/prim adduct; considering this peak to be nonspecific yields 89^{+7}_{-50}:11^{+50}_{-7} (see the text).

Comparison to Literature Data. *Experimental Data.* The tables listed in this paper contain the relevant literature data on the overall rate coefficients for the reactions of olefins with OH: most of them are total rate coefficients, k_{OH}, including addition and other channels such as H abstraction, while others are effectively only the OH addition rate, k_{add}. Finding additional evidence for the site specificity proved quite difficult because we were able to find only one other experimental study examining the site specificity of the OH addition *directly*. Feltham et al.[52] investigated the reaction of photochemically generated OH radicals with alkenes, including asymmetric alkenes, in low-temperature Ar matrices, finding that the concentration of the secondary or tertiary radical always exceeded that of the primary radical. However, these adduct concentrations are also affected by subsequent photolysis reactions, leading to carbonyl compounds; after taking formation of these carbonyls into account, no addition site preference was apparent. It is unclear whether the Ar matrix might alter the addition mechanism from the two-step gas-phase mechanism with a long-range pre-reactive complex followed by a rotation of the OH radical toward either of the addition sites. In a theoretical study, Alvarez-Idaboy et al.[24] consider the propene + OH reaction in an inert atmosphere at low pressures; they suggest that the experimental quantification of the different products for the two addition channels in these conditions might provide a definitive answer to the regioselectivity. We are unaware if such an experiment was ever attempted; the intermediate isomerization TS above the entrance channel could bias such experimental results by partial redissociation to the initial reactant π complex.

We then turned our attention to product distribution studies in reactive atmospheres because, in principle, an asymmetric

parent alkene will yield different reaction intermediates for its respective addition sites and hence might yield different final products. In atmospheric conditions, the β-hydroxy-alkyl radicals formed after addition of OH to a double bond generally react with O_2 and, given sufficiently high levels of NO, subsequently with NO forming a β-hydroxy-alkoxy radicals + NO_2. These β-hydroxy-alkoxy radicals in turn have a comparatively low barrier to dissociation[53,54] and dissociate quickly in a carbonyl compound and an α-hydroxy-alkyl radical. Unfortunately, for many simpler alkenes the α-hydroxy-alkyl radicals typically react with O_2 yielding a carbonyl compound that is the same as that formed directly from the alternative addition within the same double bond, making the two channels indistinguishable. For more complex alkenes, the chemistry after the initial addition is usually quite complex, and (often unquantified) secondary reactions such as H shifts, ring closures, nitrate formation, or multiple dissociation routes[3,38,40,42,53] make the assignment of an observed product to a specific entrance channel hard, especially because these secondary reactions probably have a different impact on the subsequent chemistry of each the different initial addition intermediates. For some monoterpenes,[2,55] several products are observed in experiments in atmospheric conditions, but the total product fractions identified are less than 50%, indicating that the product distribution is indeed highly perturbed by subsequent chemistry. Hence, the available data here is not a true measure of the initial site-specific contributions, even if we find very good agreement for some of these compounds, for example, the $(29 \pm 6)/(20 \pm 3) = 1.45$ ratio of dicarbonyl versus monocarbonyl products from limonene[56] compared to the predicted ratio $(k_{tert} + k_{sec})/(k_{tert} + k_{prim}) = 1.43$ from the SAR. Stevens et al.[57] observed evidence for OH addition on all four sites in isoprene in a mass-spectrometric study; the relative contributions were not quantified experimentally. There is a large body of literature data on the reaction products of isoprene + OH in the presence of O_2 and NO; the main products observed[58−60] are methyl vinyl ketone (32%) and methacrolein (23%) together with their coproduct formaldehyde (60%), as well as hydroxycarbonyls (15%), 3-methylfuran (5%), and nitrates (10%). Methyl vinyl ketone and methacrolein are formed after OH addition on the first and fourth carbon in isoprene, respectively, and their relative yield is in fair agreement with the SAR-predicted relative contributions for these sites (5.7 and 3.0). However, the hydroxycarbonyls $HOCH_2-CH=C(CH_3)-CHO$ and $HOCH_2-C(CH_3)=CH-CHO$ are also formed in subsequent reactions[60] of the initial adducts after OH addition on the first and fourth carbon, respectively; unfortunately, their relative yield is as yet uncertain. 3-Methylfuran[31,60] is in turn most likely formed after cyclization and H_2O loss from the hydroxyaldehydes. It is clear that the product distribution is again influenced strongly by subsequent chemistry, and direct and complete information on the relative contributions of the initial addition sites is not yet available. For the OH-initiated oxidation of α-pinene, we found good agreement between the available experimental product data and an extensive theoretical product distribution study[37] based partly on the current SAR. However, given the complexity of the degradation mechanism and the fact that α-pinene is one of the compounds with the largest deviations from the SAR (attributed in ref 37 to nonoptimal hyperconjugation stabilization due to the strained bicyclic geometry), this evidence might be less compelling.

Data in low-NO conditions, that is, where subsequent chemistry is determined by peroxy + peroxy radical chemistry, was also found to be inconclusive because it often depends on the, mostly unknown, branching ratios for the peroxy + peroxy radical reactions and might also be affected by unimolecular reactions. Cvetanovic[21] reported 65% OH addition on the outer carbon of propene based on the formation of different peroxide products, in fair agreement with the 87% predicted by our SAR. However, a theoretical study[25] suggests that Cvetanovic's results might be explained not by an initial regioselectivity but by the energetics of the subsequent O_2 chemistry.

Theoretical Work. The general mechanism of OH addition on π bonds is quite well established from quantum chemical calculations:[24−31,33−35] the OH radical first forms a T-shaped π complex with the alkene (the OH hydrogen pointing toward the alkene) through a barrierless association reaction, followed by an addition on the double bond through a TS slightly above the π-complex energy. The most recent, highest-level theoretical kinetic calculations[35] based on a two-transition-state model with an outer association TS and an inner addition TS showed that at room-temperature both have a significant impact on the rate coefficient. Our basic hypothesis describes the rate coefficient

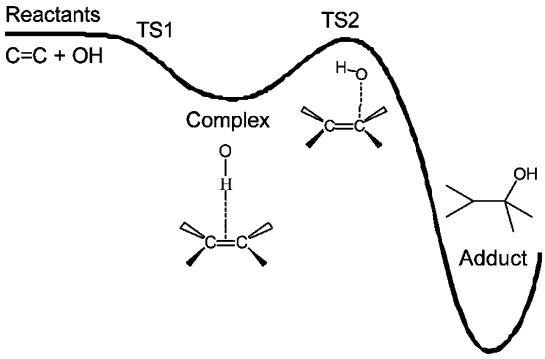

for addition as an additive contribution from each of the two addition sites within the double bond. This model clearly agrees with separate, rate-determining inner addition transition states for each of the addition sites, that is, rotating the OH radical left or right toward one of the carbons. The existence of a shared pre-addition π complex formed in a single outer TS governed by longer-range effects, however, might not be compatible with an additive site-specific model. Alternatively, the electron-density of the π bond is affected by the substituents on both sides of the double bond, and these substituents therefore affect the stability of the π complex and the outer association TS. Although the impact of substitution on the properties of the outer association TS has not been studied directly, quantum chemical calculations for OH addition on asymmetric alkenes[24,25,28,31,32,34] all show an asymmetric π complex; the energetic stability of the complex depends on the substitution. As long as the characteristics of the outer complex-forming TS are properly correlated with the (averaged) contribution of the two addition sites, a reasonable expectation for these long-range effects, our first basic hypothesis matches the general two-step addition mechanism: the site specificity is governed by the two inner addition TS, whereas the overall rate coefficient for addition depends on the two separate inner addition TS combined with the outer TS influenced by the averaged effect of both sites. Future work on the temperature and pressure dependence of the rate coefficient and site contributions might have to account for the two transition states explicitly.

Quantum chemical calculations on asymmetric alkenes might also provide support for our second hypothesis, that is, that the site-specific contribution depends nearly exclusively on the substitution around the product alkyl radical site and not on the substitution on the carbon added upon. Unfortunately, there

are relatively few theoretical studies on asymmetric alkenes + OH[24,25,28,31,32,34,57] to fall back on. Conventional wisdom tells us that substituted alkyl radicals are more stable, and combining this stabilization with a Polanyi−Evans relationship linking reaction exoergicity to barrier height would readily explain the increasing site-specific contribution k_{prim}, k_{sec}, k_{tert} with increasing product radical substitution. To test such a correlation, we performed a series of B3LYP-DFT calculations using Gaussian-98[61] for ethene, propene, isobutene, *cis*- and *trans*-2-butene, 2-Me-2-butene, and 2,3-diMe-2-butene. At that level of theory, β-hydroxy alkyl radicals are stabilized by additional substitution on the radical site, with secondary and tertiary radicals on average 1.5 and 2.2 kcal/mol below primary radicals using a 6-31G(d,p) basis set, and 1.2 and 1.8 kcal/mol using a 6-311++G(2df,2pd) basis set. Unfortunately, virtually every other quantum chemical method we applied, including Møller−Plesset, coupled-cluster, and Gaussian-type methodologies, shows a reverse stability ordering, with primary β-hydroxy alkyl radicals being the most stable, and secondary and tertiary less stable. This is also reported in the literature for propene[24,25,28] at the PMP2 and PMP4 levels of theory; the results for the cyclic *d*-limonene[34] are less conclusive because of the ring structure. We should therefore consider that the DFT results are erroneous and caused by an overestimation of the stabilization effect of substituents on the radical. In view of these results, a straightforward explanation of the site-specific relative rates based on reaction enthalpies seems unlikely. Theoretical work on the addition transition states for propene show that both transition states are very close in energy, with differences in relative energy of less than 0.4 kcal/mol;[24,25,28] the relative rates for the different addition sites are therefore strongly determined by the entropic differences between the transition states. The geometries in these studies were optimized at the MP2 level of theory, suffering greatly from spin contamination, and higher-level quantum chemical and theoretic-kinetic calculations are necessary to determine the relative contributions of the different TS in asymmetric alkenes.

Theoretical studies on conjugated alkenes, more specifically isoprene,[31,32] show that the barrier heights as well as the product radical energies are lower for the resonance-stabilized product channels compared to addition pathways for the inner carbons, favoring addition leading to resonance-stabilized adducts. Similar to propene, the barrier heights for the two addition TS leading to resonance-stabilized adducts are found to be nearly identical, with a small energetic advantage of only 0.2 kcal/mol[31] for the formation of the sec/prim adduct. Therefore, the relative contribution of these two channels is determined mainly by the relative rigidity of the TS, and rate coefficient calculations[31] show a dominance (64−69%) of the formation of the *tert/prim* resonance stabilized product radical. This distribution agrees very well with our $k_{tert/prim}/(k_{tert/prim} + k_{sec/prim})$ prediction of 66% in isoprene. Our SAR-predicted contributions of 60:5:5:30 for addition on carbons $C_1/C_2/C_3/C_4$ of isoprene are also comparable with the ratios derived in theoretical kinetic work by Stevens et al.[57] (72:<1:<1:28) and Lei et al.[62] (56:2:5:37).

Other Structure−Activity Relationships. The deviations cited in the comparisons below are calculated over the *subset* of compounds accommodated by both our SAR and the SAR being compared against. We also removed compounds used to derive the SAR from the comparison; the values for α-phellandrene and α-terpinene are corrected for H abstraction. The number of compounds in the resulting subset is indicated below.

Estimating rate coefficients for OH addition on olefins was first proposed by Ohta,[7,8] who showed that the rate coefficients for diolefins could be derived with good accuracy from summing the rate contributions from the individual double bonds as determined in experimental work on reference compounds. Estimates for conjugated alkenes were derived from the rate coefficients for analogous monoalkenes using a multiplication factor of 1.24. This early work does not clearly define a fixed set of compounds and associated rate coefficients to use as reference compounds, introducing a certain level of arbitrariness; this makes a direct comparison to our work difficult.

A structure−activity relationship developed by Atkinson et al.[9−12,15] predicts rate coefficients for the reactions of OH radicals with organic species, including mono- and polyalkenes, based on standard group rate coefficients modified by correction factors for substituents around the functional group examined. For OH addition on alkenes, addition rate coefficients can be estimated based on six standard substitution patterns; conjugated alkadienes are subdivided into four groups, each with an additional associated group rate coefficient depending on the substitution patterns. Correction factors are available for heterosubstituents around the double bonds. Compared to our SAR, the SAR by Atkinson et al.[15] yields on average slightly lower rate coefficients for addition (about 3.5% over 54 compounds); the deviation between the SAR predictions and the experimental data has a comparable average (20.2% vs 18.7%) and maximum deviation (∼60%) as our SAR. The SAR by Atkinson et al., however, does not yield site-specific addition contributions within a double bond or conjugated π system. Note that we did not include H-abstraction contributions in our comparison, even though the Atkinson et al. SAR can predict these contributions; as detailed in a later section, it is expected that H abstraction will contribute for a small extent, improving the predictions.

Pompe et al.[16] used multiple linear regression models to derive a predictive model based on six topological indices (MLR model), as well as a regression model based on variable connectivity indices (Model 2) differentiating between different hybridizations of the carbon atoms. Compared to our addition SAR, the MLR model yields slightly higher rate coefficients (by about 6% over 43 compounds) but with a higher average deviation (24.5% versus 17.3%) and maximum deviation (80%) from the experimental data. The average deviation for Model 2 is significantly larger again (29.7%),[16] but the structural interpretation of this model shows that the most important mechanisms in the OH + alkene reactions are addition to double bonds and H abstraction from allylic sites. These models do not yield site-specific addition rate coefficients.

Very recently, Pfrang et al. derived a correlation[17] and a SAR[20] for addition of OH on alkenes and nonconjugated polyalkenes, based on an extensive set of quantum chemical calculations on the energies of the highest occupied molecular orbitals and includes group reactivity factors for different types of alkyl substituents around the double bond. Compared to our work, their addition rate coefficients are significantly lower, underpredicting the experimental rate coefficients by 12% on average (46 compounds), but with a comparable average deviation (21.0% vs 19.5%) and maximum deviation (∼50%) from the experimental data as our SAR. The work by Pfrang et al.[20] also shows that the length and branching of the alkyl substituents around the double bond is expected to show a definite but small effect (≤10%) on the total rate coefficient for addition. This SAR does not yield site-specific addition contributions.

Discussion

The SAR described in this paper provides a valuable tool for accurately predicting site-specific and total rate coefficients

for the addition of OH radicals on (poly)alkenes at 298 K as needed in the construction of atmospheric chemistry models and the elucidation of degradation and product formation mechanisms of volatile organic compounds. The SAR is based on the experimental rate coefficients of only 3 (for isolated double bonds) and 6 (for conjugated alkadienes) reference compounds (see Table 1), yet the average deviation between the total experimental rate coefficient and the predicted addition rate coefficient using the SAR site-specific rate coefficients (see Table 2) for the 64 compounds in Tables 3−5 is only 13% without the need of fitted SAR parameters (Figure 4). In this section, we will discuss certain aspects of the SAR in more detail, in particular systematic deviations and trends and deviations for compounds that are apparently predicted with less accuracy.

Ring Strain, Conformers, and Steric Hindrance. The average deviations for regular and monocyclic alkenes and for (most of the) conjugated alkadienes is about 10%. The average error of the predictions for bicyclic compounds is significantly larger, ∼24%, and includes some of the compounds with the largest deviations. This can for the largest part be attributed to changes in the ring strain in these bicylic compounds: the sp^2-sp^2 hybridization of the double-bonded carbons changes to a sp^3-sp^2 hybridization, with corresponding changes in bond angles and lengths. In some cases this reduces the ring strain, especially because the sp^2-carbon-centered radical easily deforms from its planar geometry to reduce overall strain, whereas in other cases ring strain increases upon addition of OH. In the addition transition states, these ring strain changes will already be partly present, affecting the rate of addition to a certain extent. Monocyclic compounds (see, e.g., cyclopentene, -hexene, and -heptene) are hardly affected, so the effect is clearly not overly large, but the highly strained nature of some bicyclic compounds makes them more sensitive to such geometric modifications. We are not aware of quantum chemical or theoretical-kinetic work studying the effect of ring strain for OH + olefine reactions in detail, but we can illustrate the effects with some exploratory B3LYP-DFT/6-31G(d,p) relative energy calculations on *β*-pinene and isobutene, which have a similar alkene substructure.

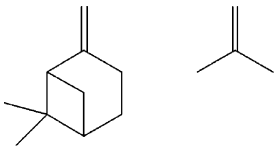

β-pinene iso-butene

The well depths for OH addition forming a tertiary radical are nearly identical (within 1 kcal/mol) for *β*-pinene + OH and isobutene. In contrast, the OH adduct with a primary radical site is about 3 kcal/mol less stable for *β*-pinene compared to isobutene; clearly, the geometry change of the carbon within the ring structure of *β*-pinene is energetically not favorable. This is expected to impact the barrier height and rigidity, and hence addition on the endocyclic carbon is probably even less important than that currently predicted by the SAR. Similar energetic and entropic effect for other (bi)cyclic compounds will also cause deviations between strained and strain-free, resulting in a larger error between experiment and SAR. Note that here the underprediction of the rate coefficient by the SAR for *β*-pinene is due to the lack of H-abstraction contributions in our prediction. For bicyclo-[2.2.2]-2-octene, where the SAR overpredicts the rate of addition by 47%, we also expect a large influence of ring strain.

Sabinene is an exceptional case, defying all attempts at predicting its rate coefficients with OH, NO_3, or O_3 using SARs. The most likely explanation is that the proximity of a strained three-membered ring to the double bond allows for additional, nontraditional reaction pathways, such as concerted addition/ring breaking reactions or even addition or abstraction reactions near the three-membered ring enhanced by allyl stabilization of the reaction product radical. For this reason, we expect that sabinene will have to be treated explicitly outside any SAR treatment.

In our derivation of the SAR, we quantified k_{sec} from the averaged rate coefficients for *cis*- and *trans*-2-butene. Using the rate coefficient for the trans conformer seems more appropriate for most noncyclic compounds, whereas *cis*-conformers might be a better model for endocyclic double bonds. The difference between $2 \times k_{sec}$ and the specific rate coefficients for *cis*- and *trans*-2-butene, however, is only about 7%, comparable to the statistical uncertainty between our predictions and the experimental data. Also, ring strain is expected to have a larger impact on the rate coefficient than the 7% difference with the averaged k_{sec}. Hence, at the present time the use of an average over both conformers is sufficiently accurate and eliminates the need for additional parameters in the SAR.

Francisco-Márquez et al.[32] studied the effect of cis and trans conformers of conjugated alkadienes in theoretical calculations on butadiene and isoprene. They found lower barriers for addition in the cis conformers, with a larger effect for the inner carbons. Hence, the existence of cis and trans conformers of alkadienes could affect the rate coefficients as well as the site specificity. At 298 K, the population fraction of *cis*-alkadiene conformers is only a few percent, such that it will probably not impact our predictions significantly, but future work on higher temperature predictions and temperature dependencies might have to include cis−trans conformism explicitly.

The compound where the SAR prediction shows the largest relative deviation is α-pinene, with an overestimation of 63% (experimental: 5.23×10^{-11} cm^3 s^{-1}; SAR prediction: 8.51×10^{-11} cm^3 s^{-1}). A tentative explanation based on steric hindrance is that the $>C(CH_3)_2$ bridge hovering over the double bond is partly blocking the formation of the pre-reactive *π* complex for OH addition on the syn side of the substituted bridge. In this particular case, the rigid bicyclic structure would prevent substituent reorientation to accommodate the approach of the OH radical toward the double bond; the steric hindrance would then reduce the addition rate coefficient. However, the deviation for α-pinene might also be caused by strain in the ring structure, similar to *β*-pinene, as we find in exploratory B3LYP-DFT/6-31G(d,p) calculations that the stability of the OH adducts with tertiary radical site is reduced by 1−2 kcal/mol (depending on syn or anti orientation relative to the $>C(CH_3)_2$ bridge) in comparison to 2-Me-2-butene with an identical but unstrained alkene substructure. We attributed the difference in adduct well

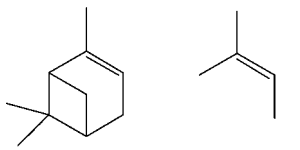

α-pinene 2-Me-2-butene

depth earlier[37] to a suboptimal hyperconjugation overlap toward the carbon in the adjacent strained four-membered ring in the tertiary product radical, such that it behaves more like a secondary radical. The addition pathway leading to the tertiary product radical, k_{tert}, is the largest contribution in the SAR

prediction, and a lowering of the rate coefficient for this channel due to even a slight increase of the barrier height or TS rigidity would bring the SAR prediction much closer to the experimental values. More advanced theoretical work is needed to conclude whether steric hindrance can be an issue in any of the compounds considered here or that the energetic and entropic impact of ring strain is the dominant reason for the larger scatter found for bicyclic compounds.

H Abstraction. It is generally accepted that H abstraction is a minor channel in the reaction of alkenes + OH; the good agreement between our SAR addition rate coefficients and the measured total rate coefficients concurs with this assertion. However, as already indicated earlier, the stability of (super)-allyl stabilized radicals formed after H abstraction significantly promotes H-abstraction rates: for α-terpinene and α-phellandrene, H abstraction was even measured directly[6] to contribute for 30 ± 7% and 27 ± 10%, respectively, and thereby accounting for most of the difference between our SAR predictions for addition and the measured total rate coefficient. H abstraction from 1,3-and 1,4-cylohexadiene is somewhat lower because of the lack of tertiary hydrogen sites and measured at 10−15%[6,63,64] and 7%,[63] respectively. For 3-methyl-1-butene, abstraction of the tertiary hydrogen was estimated at 5−10%.[65] For compounds lacking a superallyl-enhanced or a tertiary H-abstraction site, contributions of H abstraction are now generally considered minor, <10%, despite some earlier work with higher contributions.[49,66] Tully[67] found that H abstraction is the dominant channel at temperatures above 650 K for 1-butene + OH; extrapolation to room temperatures suggests an H-abstraction contribution of 2−3%, in agreement with earlier experimental work by Atkinson et al.[68] suggesting an upper limit of 10%. Some other compounds, such as ethene,[69] isoprene,[70] and 1,3,5-cycloheptatriene,[64] were also found to have a negligible H-abstraction contribution. The moderate increase in the experimental total rate coefficients for the series [1-butene, 1-pentene, 1-hexene, 1-heptene] (see Table 3) also indicates that each additional $-CH_2-$ unit in the alkyl substituent contributes to the rate coefficient; the theoretical work by Pfrang et al.[19,20] shows that the rate of addition is not affected appreciably (2−3%) upon elongation of the alkyl substituent beyond a $-CH_3$ methyl group, suggesting that the increase is due to H abstraction on the alkyl chain.

Even with contributions of a few percent (<10−15%), H abstraction would account for a large fraction of the residual errors found in the comparison between our SAR-predicted addition and measured total rate coefficients. In particular, it would explain the apparent curvature in the k_{exp} versus k_{SAR} plot in Figure 4 where larger compounds with higher rate coefficients are typically underestimated: precisely, these larger, more branched compounds contain the most promising H-abstraction sites including tertiary hydrogens and hydrogens next to conjugated π systems shown experimentally to contribute significantly.[6] To test the potential impact of H abstraction, we generated predicted total rate coefficients $k_{tot} = k_{SAR} + k_{abstr}$ by summing the addition rate coefficient as predicted by the current SAR, k_{SAR}, with predicted H-abstraction rate coefficients k_{abstr}. The k_{abstr} were obtained by summing all site-specific abstraction rate coefficients, $k_{abstr,i}$, with each hydrogen abstraction site characterized based on its immediate environment as outlined earlier by Vereecken and Peeters:[71] primary, secondary, and tertiary hydrogen sites are distinguished, as well as the presence/absence of allyl-resonance or superallyl resonance stabilization in the product radical. The resulting k_{tot} versus k_{exp} correlation is much more linear, with larger compounds being significantly closer to a 1:1 ideal correlation. Also, the horizontal artefacts in the lower-left corner of Figure 4, caused by an identical k_{add} prediction for different compounds with slightly different k_{exp}, are tilted to nearly match the ideal 1:1 correlation. As such, attributing the bulk of the remaining residual errors between our SAR and the experimental data to H abstraction seems a promising avenue. Still, we refrain from including the H-abstraction contributions in the present paper because the current treatment of the H abstraction is too rudimentary. We have shown earlier that the H-abstraction rate is correlated nonlinearly to the C−H bond strength[72,73] and, for example, using a single $k_{abstr,tert}$ value for all tertiary sites is not sufficiently accurate. Also, for H abstraction enhanced by resonance stabilization, one should consider the substitutions on all product radical sites; similar to the OH addition discussed in the current SAR, one expects that substitution on the second (third) resonance radical site will have a different impact on the H-abstraction rate as the initial abstraction site. The accuracy of the current simple treatment deteriorates further when considering (bi)cyclic compounds, where ring strain can significantly alter bond strengths and abstraction rates.[47,71] Finally, the increase in rate coefficient for the series [1-butene, 1-pentene, 1-hexene, 1-heptene], about $2-4 \times 10^{-12}$ cm^3 s^{-1} per additional CH_2 group, is larger than that predicted for typical H-abstraction rate coefficients for secondary $-CH_2-$ hydrogens, $\sim 1.0-1.5 \times 10^{-12}$ cm^3 s^{-1}, suggesting that perhaps the pre-reactive π complex formation also enhances H-abstraction rates. The lack of accurate H-abstraction contributions is one of the reasons we opted not to numerically optimize the basic SAR parameters k_{prim}, k_{sec}, and so forth at this time because doing so would shift part of the uncertainty on the H-abstraction contribution into the addition rate SAR parameters, thereby also conceptually blending contributions for addition and abstraction within these parameters.

Heterosubstituents. With the exception of halogenated compounds, there is little systematic data available concerning OH addition on heterosubstituted (poly)alkenes. This is unfortunate because, for example, oxygenated compounds and particularly hydroxy- and carbonyl-substituted compounds are commonly formed in the atmospheric oxidation of hydrocarbons; examples include methylvinylketone, methacrolein, terpinen-4-ol, and (meth)acrylic acid. The polyunsaturated terpenoids, in particular, have the potential to form stable but very reactive unsaturated oxygenated intermediates. The impact of hydroxy or carbonyl substituents in an alkene on the rate coefficient for addition is difficult to predict a priori. α-Hydroxy substituents tend to stabilize an alkyl radical (see, e.g., the rate coefficients for ethanol + OH vs ethane + OH), but the -enol compounds needed to observe this effect usually rearrange to the more stable keto form. Vinoxy resonance in the product radical formed after OH addition on a >C═C−C═O compound is not likely to enhance the addition rate significantly, given that the second radical site (the carbonyl oxygen) is a primary site, that $k_{sec/prim}$ and $k_{tert/prim}$ are nearly identical to k_{sec} and k_{tert}, and that delocalisation in vinoxy resonance is less pronounced than in allyl resonance. However, the formation of H bonds between the OH radical and the >C═O, −OH, or −COOH bond could significantly affect the stability of the pre-reactive π complex and hence the rate of OH addition. We currently do not include heterosubstituents in the structure−activity relationship developed here, until more information is available, both experimentally and theoretically, on the impact of H bonding on the addition pathways of OH radicals onto alkenes.

Conclusions

In this work we developed a novel, quantitative SAR for the prediction of site-specific rate coefficients for the addition of OH to alkenes. The deduction of the SAR rests on two basic hypotheses: (*i*) the overall rate coefficient for addition is equal to the sum of the site-specific rate coefficients of all addition sites and (*ii*) the site-specific rate coefficient is determined mostly by the substitution around the product radical site. From these hypotheses, a site-specific SAR is derived based on the experimental rate coefficients of 9 alkenes and conjugated alkadienes with OH, showing very good predictive capabilities across a diverse set of 65 compounds, without any adjustable parameters. For most (poly)alkenes and conjugated alkadienes, the SAR-predicted total rate constant is within <15% of the experimental values; possible sources of error include H-abstraction contributions, and ring strain in bicyclic compounds.

The site specificity of the SAR is validated against direct experimental measurement on a set of compounds including both asymmetric alkenes as well as conjugated alkadienes. The experiments show irrevocably that the product distribution of the hydroxy-alkyl product radicals is well predicted by the SAR.

Acknowledgment. This work was carried out in part in the frame of the Belgian research program Science for Sustainable Development of the Belgian Science Policy Office (project SD/AT/03A).

References and Notes

(1) Guenther, A.; Hewitt, C. N.; Erickson, D.; Fall, R.; Geron, C.; Graedel, T.; Harley, P.; Klinger, L.; Lerdau, M.; McKay, W. A.; Pierce, T.; Schjoles, B.; Steinbrecher, R.; Tallamraju, R.; Taylor, J.; Zimmerman, P. K. *J. Geophys. Res.* **1995**, *100*, 8873.

(2) Atkinson, R. *J. Phys. Chem. Ref. Data* **1997**, *26*, 215.

(3) Atkinson, R. *Atmos. Environ.* **2000**, *34*, 2063.

(4) Warneck, P. *Chemistry of the Natural Atmosphere*, International Geophysics Series; Academic Press Inc.: New York, 1988; Vol. 41.

(5) Finlayson-Pitts, B. J.; Pitts, J. N., Jr. *Chemistry of the Upper and Lower Atmosphere*; Academic Press: San Diego, CA, 2000.

(6) Peeters, J.; Vandenberk, S.; Piessens, E.; Pultau, V. *Chemosphere* **1999**, *6*, 1189.

(7) Ohta, T. *Int. J. Chem. Kinet.* **1984**, *16*, 879.

(8) Ohta, T. *J. Phys. Chem.* **1983**, *87*, 1209.

(9) Atkinson, R.; Ashmann, S. M. *Int. J. Chem. Kinet.* **1983**, *15*, 1169.

(10) Atkinson, R.; Ashmann, S. M. *Int. J. Chem. Kinet.* **1984**, *16*, 1175.

(11) Atkinson, R. *Chem. Rev.* **1986**, *86*, 69.

(12) Atkinson, R.; Arey, J. *Chem. Rev.* **2003**, *103*, 4605.

(13) Atkinson, R. *J. Phys. Chem. Ref. Data* **1994**, *monograph 2*.

(14) Atkinson, R. *Int. J. Chem. Kinet.* **1987**, *19*, 799.

(15) Kwok, E. S. C., Atkinson, R. *Atmos. Environ.* **1995**, *29*, 1685.

(16) Pompe, M.; Veber, M.; Randic, M.; Balaban, A. T. *Molecules* **2004**, *9*, 1160.

(17) King, M. D.; Canosa-Mas, C. E.; Wayne, R. P. *Phys. Chem. Chem. Phys.* **1999**, *1*, 2231.

(18) King, M. D.; Canosa-Mas, C. E.; Wayne, R. P. *Phys. Chem. Chem. Phys.* **1999**, *1*, 2239.

(19) Pfrang, C.; King, M. D.; Canosa-Mas, C. E.; Wayne, R. P. *Atmos. Environ.* **2006**, *40*, 1170.

(20) Pfrang, C.; King, M. D.; Canosa-Mas, C. E.; Wayne, R. P. *Atmos. Environ.* **2006**, *40*, 1180.

(21) Cvetanovic, R. J. *12th Int. Symp. on Free Radicals*, unpublished, Laguna Beach, CA, January 1976.

(22) Singleton, D. L.; Cvetanovic, R. J. *J. Am. Chem. Soc.* **1976**, *98*, 6812.

(23) Davey, J. B.; Greenslade, M. E.; Marshall, M. D.; Lester, M. I.; Wheeler, M. D. *J. Chem. Phys.* **2004**, *121*, 3009.

(24) Alvarez-Idaboy, J. R.; Díaz-Acosta, I.; Vivier-Bunge, A. *J. Comput. Chem.* **1998**, *811*, 811.

(25) Díaz-Acosta, I.; Alvarez-Idaboy, J. R.; Vivier-Bunge, A. *Int. J. Chem. Kinet.* **1999**, *31*, 29.

(26) Alvarez-Idaboy, J. R.; Mora-Diez, N.; Vivier-Bunge, A. *J. Am. Chem. Soc.* **2000**, *122*, 3715.

(27) Hippler, H.; Viskolcz, B. *Phys. Chem. Chem. Phys.* **2000**, *2*, 3591.

(28) Selçuki, C.; Aviyente, V. *J. Mol. Model.* **2001**, *7*, 398.

(29) Piqueras, M. C.; Crespo, R.; Nebot-Gil, I.; Tomás, F. *J. Mol. Struct.: THEOCHEM* **2001**, *537*, 199.

(30) Liu, G.-X.; Ding, Y.-H;, Li, W.-S.; Fu, Q.; Huang, X.-R.; Sun, C.-C.; Tang, A.-C. *Phys. Chem. Chem. Phys.* **2002**, *4*, 1021.

(31) Francisco-Márquez, M.; Alvarez-Idaboy, J. R.; Galano, A.; Vivier-Bunge, A. *Phys. Chem. Chem. Phys.* **2003**, *5*, 1392.

(32) Francisco-Márquez, M.; Alvarez-Idaboy, J. R.; Galano, A.; Vivier-Bunge, A. *Phys. Chem. Chem. Phys.* **2004**, *6*, 2237.

(33) Zhu, R. S.; Park, J.; Lin, M. C. *Chem. Phys. Lett.* **2005**, *408*, 25.

(34) Ramírez-Ramírez, V. M.; Nebot-Gil, I. *Chem. Phys. Lett.* **2005**, *409*, 23.

(35) Greenwald, E. E.; North, S. W.; Georgievskii, Y.; Klippenstein, S. J. *J. Phys. Chem. A* **2005**, *109*, 6031.

(36) Vereecken, L.; Peeters, J. *J. Phys. Chem. A* **2000**, *104*, 11140.

(37) Peeters, J.; Vereecken, L.; Fantechi, G. *Phys. Chem. Chem. Phys.* **2001**, *3*, 5489.

(38) Vereecken, L.; Peeters, J. *J. Phys. Chem. A* **2004**, *108*, 5197.

(39) Greenwald, E. E.; Park, J.; Anderson, K. C.; Kim, H.; Reich, B. J. E.; Miller, S. A.; Zhang, R.; North, S. W. *J. Phys. Chem. A* **2005**, *109*, 7915.

(40) Vereecken, L.; Peeters, J. *J. Chem. Phys.* **2003**, *119*, 5159.

(41) Fantechi, G.; Vereecken, L.; Peeters, J. *Phys. Chem. Chem. Phys.* **2002**, *4*, 5795.

(42) Dibble, T. S. *J. Phys. Chem. A* **2004**, *108*, 2199.

(43) Peeters, J.; Boullart, W.; Van Hoeymissen J. In *Proc. Eurotrac Symp '94*; Borrell, P. M., Borrell, P., Cvitaš, T., Seiler W., Eds.; SPB Academic Publishers: The Hague, The Netherlands, 1994; pp 110−114.

(44) Peeters, J.; Boullart, W.; Pultau, V.; Vandenberk, S. In *Proceedings of EUROTRAC symposium '96*; Borrell, P. M., Borrell, P., Cvitaš, T., Kelly, K., Seiler W., Eds.; Computational Mechanics Publications: Southampton, U.K., 1996; pp 471−475.

(45) Boullart, W.; Van Hoeymissen, J.; Pultau, V.; Dehaen, W.; Peeters, J. In *Air pollution research report 57: Homogeneous and heterogeneous chemical processes in the troposphere 1996*; Mirabel, Ph., Ed.; European Commission: Brussels, 1996; pp 212−217.

(46) Atkinson, R.; Baulch, D. L.; Cox, R. A.; Hampson, R. F.; Kerr, J. A.; Troe, J. *Atmos. Environ.* **1992**, *26A*, 1187.

(47) Vereecken, L.; Peeters, J. *Phys. Chem. Chem. Phys.* **2002**, *4*, 467.

(48) Spencer, J. E.; Glass, G. P. *Chem. Phys.* **1976**, *15*, 35.

(49) Bierman, H. W.; Harris, G. W.; Pitts, J. N., Jr. *Adv. Photochem.* **1979**, *11*, 375.

(50) Pultau, V. Ph.D. Thesis, K.U.Leuven, 1996.

(51) Vandenberk, S. Licentiate Thesis, K.U.Leuven, 1996.

(52) Feltham, E. J.; Almond, M. J.; Marston, G.; Wiltshire, K. S.; Goldberg, N. *Spectrochimica Acta, Part A* **2000**, *56*, 2589.

(53) Peeters, J.; Fantechi, G.; Vereecken. L. *J. Atmos. Chem.* **2004**, *48*, 59.

(54) Atkinson, R. *Int. J. Chem. Kinet.* **1997**, *29*, 99.

(55) Atkinson, R.; Arey, J. *Atmos. Environ.* **2003**, *37* (Suppl. 2), S197.

(56) Hakola, H.; Arey, J.; Aschmann, S. M.; Atkinson, R. *J. Atmos. Chem.* **1994**, *18*, 75.

(57) Stevens, P. S.; Seymour, E.; Li, W. *J. Phys. Chem. A* **2000**, *104*, 5989.

(58) Carter, W. P. L.; Atkinson, R. *Int. J. Chem. Kinet.* **1996**, *28*, 497.

(59) Zhao, J.; Zhang, R.; Fortner, E. C.; North, S. W. *J. Am. Chem. Soc.* **2004**, *126*, 2686.

(60) Baker, J.; Arey, J.; Atkinson, R. *Environ. Sci. Technol.* **2005**, *39*, 4091.

(61) Frisch, M. J.; Trucks, G. W.; Schlegel, H. B.; Scuseria, G. E.; Robb, M. A.; Cheeseman, J. R.; Zakrzewski, V. G.; Montgomery, J. A., Jr.; Stratmann, R. E.; Burant, J. C.; Dapprich, S.; Millam, J. M.; Daniels, A. D.; Kudin, K. N.; Strain, M. C.; Farkas, O.; Tomasi, J.; Barone, V.; Cossi, M.; Cammi, R.; Mennucci, B.; Pomelli, C.; Adamo, C.; Clifford, S.; Ochterski, J.; Petersson, G. A.; Ayala, P. Y.; Cui, Q.; Morokuma, K.; Malick, D. K.; Rabuck, A. D.; Raghavachari, K.; Foresman, J. B.; Cioslowski, J.; Ortiz, J. V.; Stefanov, B. B.; Liu, G.; Liashenko, A.; Piskorz, P.; Komaromi, I.; Gomperts, R.; Martin, R. L.; Fox, D. J.; Keith, T.; Al-Laham, M. A.; Peng, C. Y.; Nanayakkara, A.; Gonzalez, C.; Challacombe, M.; Gill, P. M. W.; Johnson, B. G.; Chen, W.; Wong, M. W.; Andres, J. L.; Head-Gordon, M.; Replogle, E. S.; Pople, J. A. *Gaussian 98*, revision A.9; Gaussian, Inc.: Pittsburgh, PA, 1998.

(62) Lei, W.; Derecskei-Kovacs, A.; Whang, R. *J. Chem. Phys.* **2000**, *113*, 5354.

(63) Ohta, T. *Int. J. Chem. Kinet.* **1984**, *16*, 1495.

(64) Tuazon, E. C.; Aschmann, S. M.; Nguyen, M. V.; Atkinson, R. *Int. J. Chem. Kinet.* **2003**, *35*, 415.

(65) Atkinson, R.; Tuazon, E. C.; Aschmann, S. M. *Int. J. Chem. Kinet.* **1998**, *30*, 577.

(66) Atkinson, R.; Perry, R. A.; Pitts, J. N., Jr. *J. Chem. Phys.* **1977**, *67*, 3170.

(67) Tully, F. P. *Chem. Phys. Lett.* **1988**, *143*, 510.

(68) Atkinson, R.; Tuazon, E. C.; Carter, W. P. L. *Int. J. Chem. Kinet.* **1985**, *17*, 725.

(69) Bartels, M.; Hoyermann, K.; Sievert, R. *19th Symp. (Int.) Combust.* **1982**, 61.

(70) Atkinson, R.; Ashmann, S. M.; Tuazon, E. C.; Arey, J.; Zielinska, B. *Int. J. Chem. Kinet.* **1989**, *21*, 593.

(71) Vereecken, L.; Peeters, J. *Chem. Phys. Lett.* **2001**, *333*, 162.

(72) Peeters, J.; Vandenberk, S.; Pultau, V.; Boullart, W.; Van Hoeymissen, J.; Fantechi, G.; Vereecken, L. *Structure−Activity Relationships and Correlations for Some Key Reactions in Atmospheric Chemistry*, Faraday Discussion 130 - Atmospheric Chemistry; Leeds, U.K., April 2005.

(73) Vereecken, L.; Vandenberk, S.; Peeters, J. *Correlating H-abstraction by OH to C−H bond strengths: conjugation versus resonance stabilisation*", 17th Symposium (Int.) Gas Kinetics; Essen, Germany, August 2002.